FEBS Letters 553 (2003) 328–332 FEBS 27687

A binding event converted into a folding event

F.M. Martín-Sierra[a], A.M. Candel[a], S. Casares[a], V.V. Filimonov[a,b], J.C. Martínez[a,*], F. Conejero-Lara[a,*]

[a] *Departamento de Química Física e Instituto de Biotecnología, Facultad de Ciencias, Universidad de Granada, 18071 Granada, Spain*
[b] *Institute of Protein Research of the Russian Academy of Sciences, Puschino, Moscow Region 142292, Russia*

Received 21 July 2003; revised 9 September 2003; accepted 10 September 2003

First published online 25 September 2003

Edited by Thomas L. James

Abstract **We have designed a chimeric protein by connecting a circular permutant of the α-spectrin SH3 domain to the proline-rich decapeptide APSYSPPPPP with a three-residue link. Our aim was to obtain a single-chain protein with a tertiary fold that would mimic the binding between SH3 domains and proline-rich peptides. A comparison of the circular-dichroism and fluorescence spectra of the purified chimera and the SH3 circular permutant showed that the proline-rich sequence occupies the putative SH3 binding site in a similar conformation and with comparable interactions to those found in complexes between SH3 and proline-rich peptides. Differential scanning calorimetry indicated that the interactions in the binding motif interface are highly cooperative with the rest of the structure and thus the protein unfolds in a two-state process. The chimera is more stable than the circular permutant SH3 by 6–8 kJ mol^{-1} at 25°C and the difference in their unfolding enthalpy is approximately 32 kJ mol^{-1}, which coincides with the values found for the binding of proline-rich peptides to SH3 domains. This type of chimeric protein may be useful in designing SH3 peptide ligands with improved affinity and specificity.**

Key words: Src-homology region 3 domain; Proline-rich peptide; Protein–ligand binding; Protein folding; Protein stability; Differential scanning calorimetry

1. Introduction

Src-homology region 3 (SH3) domains are probably the most widely known modules for molecular recognition [1], which has resulted in their becoming important targets for ligand design. They interact with proline-rich sequences, with a preserved PxxP binding motif, adopting a poly-proline II (PPII) helical conformation. The binding site of SH3 domains consists of a hydrophobic surface containing three shallow pockets defined by preserved aromatic residues [2]. Two of the pockets accommodate each of the prolines, accompanied by a hydrophobic residue in the PxxP motif. The third pocket, known as the 'specificity pocket', is flanked by the RT and n-src loops, which play an important role in both the affinity and the specificity of the interaction [1].

An understanding of the thermodynamic determinants of the affinity and specificity of the SH3 domains is of particular importance in being able to predict ligands for proteins of particular interest and, in some cases, to design ligands for the specific inhibition of interactions in vivo. The thermodynamic dissection of protein–ligand interactions involves laborious titration experiments with systematically modified ligands, usually carried out by isothermal titration calorimetry (ITC) [3]. In the case of SH3 domains this implies the use of considerable quantities of protein and expensive synthetic peptides, which may explain why only a few calorimetric studies into the binding between SH3 domains and proline-rich peptides have been undertaken [4–7].

The folding properties of SH3 domains are also well characterised both by experimental [8–14] and computational methods [15–18]. Although the folding kinetics of this family of small domains appears to be mainly determined by the chain topology of the native state [14,15,19,20], it has been shown that this topology can be changed in the SH3 domain of α-spectrin by circular permutation without affecting the overall fold [19,21]. The RT-loop of one of the circular permutants, S19P20s, is open (cf. Fig. 1A) and the new C-terminus is quite close to the binding site for proline-rich peptides, adjacent to the specificity pocket. This topology allows us to engineer chimeric variants of this circular permutant with an extended chain sequence that mimics in its fold the interactions with proline-rich peptides. On the basis of this approach it should be possible to design new interactions at the domain–ligand interface by simple site-directed mutagenesis in these chimeras and to characterise the effects produced by studying the thermodynamics of their folding–unfolding.

We describe here the design, isolation and characterisation of a chimeric protein obtained by connecting the circular permutant S19P20s of the SH3 domain of α-spectrin to the sequence of a proline-rich ligand designed previously for the Abl-SH3 domain [22]. The results highlight the common thermodynamic features between protein–ligand binding and protein folding.

2. Materials and methods

The gene encoding the chimeric proteins was obtained by polymerase chain reaction (PCR) [23], extending the 3′-end DNA sequence of the circular permutant S19P20s to obtain the following amino acid

*Corresponding author. Fax: (34)-958-272879.
E-mail addresses: jcmh@ugr.es (J.C. Martínez), conejero@ugr.es (F. Conejero-Lara).

Abbreviations: SH3, Src-homology region 3; p41, decapeptide of sequence APSYSPPPPP; S19P20s, circular permutant of the α-spectrin SH3 domain cut between positions S19 and P20 with its N- and C-ends linked; SPCp41, chimeric S19P20s elongated from its C-terminus with a three-residue link of sequence DGN plus the p41 sequence; DSC, differential scanning calorimetry; CD, circular dichroism

0014-5793/03/$22.00
doi:10.1016/S0014-5793(03)01038-X

sequence: MGPREVTMKKGDILTLLNSTNKDWWKVEVNDRQGFVPAAYVKKLDSGTGKELVLALYDYQEKSxxxAPSYSPPPPP, where the underlined residues are the new amino acids added to the C-terminus of the original S19P20s sequence and xxx represents a two- or three-residue connection of variable composition. The DNA fragments were cloned into a pBAT4 plasmid [24] and expressed into *Escherichia coli* BL21/DE3 (Novagen). The proteins were purified as described elsewhere [25].

Prior to the experiments the samples were thoroughly dialysed against the appropriate buffers. Protein concentration was measured using extinction coefficients determined by Gill and von Hippel's method [26].

Differential scanning calorimetry (DSC) experiments were performed in a VP-DSC microcalorimeter (Microcal) at a scan rate of 90°C/h. The protein concentration in all DSC experiments was ≈1 mg/ml. The temperature dependence of the molar partial heat capacity (C_p) of SH3 was calculated from the DSC data and analysed using Origin 6.1 (OriginLab). C_p curves were fitted by a non-linear least-squares method using the two-state unfolding model as described elsewhere [19].

Titration experiments following the change in intensity of tryptophan fluorescence were carried out to monitor the binding of decapeptide p41 to the SH3 variants. Protein samples were thermostatised at 25°C in the cuvette of the fluorimeter at a concentration of ≈25 μM. Fluorescence spectra were recorded between 305 and 400 nm at different p41 concentrations from 0 to ≈1 mM. The excitation wavelength was 298 nm. The titration curves were analysed as described elsewhere [22].

Circular dichroism (CD) measurements were made in a temperature-controlled Jasco J-715 spectropolarimeter. Far-UV and near-UV CD spectra were recorded at 25°C in 20 mM glycine at pH 3.0 using cuvettes of 1 and 5 mm path length, respectively. Sample concentrations were ≈0.2–0.25 mg/ml for the far-UV and ≈2–2.5 mg/ml for the near-UV spectra. Baseline spectra obtained with pure buffer were subtracted for all spectra. The CD signal was expressed as molar ellipticity for the sake of comparison.

The thermal unfolding of S19P20s and SPCp41 was followed by recording the CD signal in both the far-UV (234 nm) and near-UV (295 nm) ranges at different temperatures between 5 and 95°C. The thermal profiles were corrected by subtracting the profiles obtained with pure buffers under identical conditions. The unfolding profiles were analysed according to the two-state model as reported elsewhere [27].

Computer analysis, structural alignment and modelling of protein structures were performed with the programme Swiss PDB viewer [28].

3. Results and discussion

The aim of this work was to design a single-chain chimeric protein that would mimic in its tertiary fold the typical interactions between proline-rich peptides and SH3 domains. Our first step was to make a computer model of this chimera using the crystal structure of the complex between the Abl-SH3 domain and the decapeptide p41 as a template [29]. Initially, we aligned the crystal structures of the Abl-SH3 domain in its complex with p41 (PDB: 1BBZ) and the circular permutant S19P20s (PDB: 1TUC) [21]. The root mean square deviation (RMSD) for all the backbone atoms was 1.37 Å. The main side chains in the consensus binding site of the SH3 domains were well conserved between Abl-SH3 and S19P20s (Tyr7, Phe9, Trp36, Trp47, Pro49 and Tyr52 for Abl-SH3, versus Tyr57, Tyr59, Trp24, Phe35, Pro37 and Tyr40 in S19P20s) and the spatial arrangement of the side chains was very similar for all of them (Fig. 1B). Subsequently we made a model of the complex between p41 and S19P20s by replacing the Abl-SH3 domain with S19P20s and finally we connected the S19P20s and p41 main chains with a short link of two to three residues, as illustrated in Fig. 1B. No clashes in the model were found. We did not attempt to model any additional interactions involving the two to three residues link. For this link we tried several sequences. The designed chimeras were cloned and expressed in *E. coli* and purified to homogeneity as stated in Section 2.

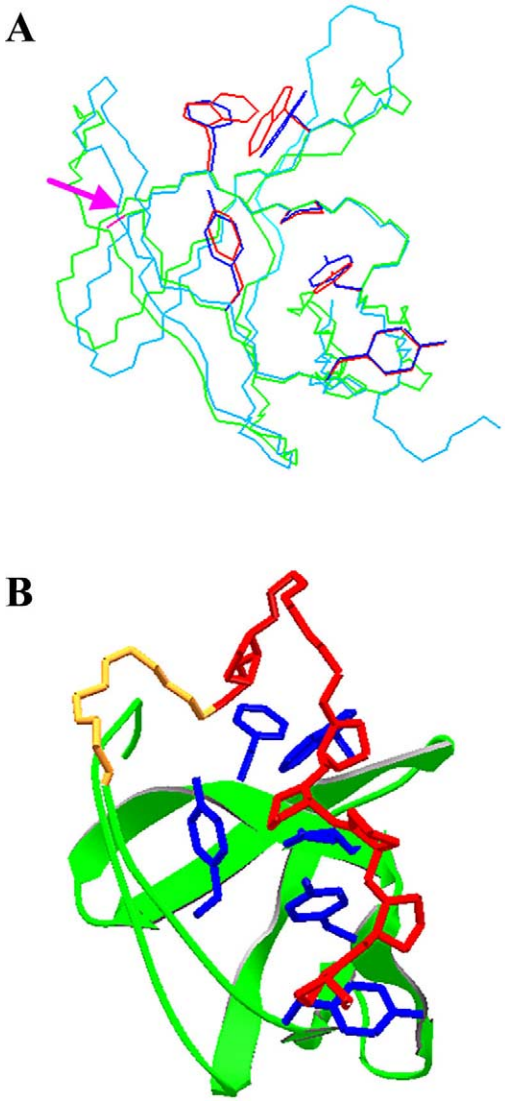

Fig. 1. A: Schematic view of the backbone chains in the alignment between the crystal structures of the Abl-SH3 domain in its complex with the decapeptide p41 (cyan) (PDB: 1BBZ) [29] and the circular permutant S19P20s (green) (PDB: 1TUC) [21]. The side chains forming the SH3 binding site have been highlighted for both domains (Abl-SH3 in red and S19P20s in blue). The arrow indicates the location of the C-terminal end in S19P20s. B: Schematic view showing a model of the structure of the chimeric domain SPCp41. The chain sequence corresponding to S19P20s is represented with ribbons. The decapeptide p41 and the backbone of the three-residue link connecting it with the S19P20s chain are coloured red and orange, respectively. The side chains of residues in the SH3 domain interacting with the p41 sequence are shown in blue.

We made preliminary tests of the thermal stability of all the chimeric proteins compared to S19P20s by running single DSC experiments in 20 mM glycine at pH 3.5. All the chimeras were more stable than S19P20s by 5–10°C, suggesting the formation of stabilising interactions between the SH3 domain and the extended sequence. The most stable chimera contained the link GDN and the deletion of K62, close to the

C-terminus in the S19P20s sequence. This deletion was intended to release any possible constraints produced by charge–charge interactions in the region of the link. We named this chimera SPCp41.

To characterise the conformation of the extended chain sequence within SPCp41 we measured the CD spectra of SPCp41, S19P20s and the isolated p41 peptide at pH 3.0 and 25°C (Fig. 2) in both the far-UV (panel A) and near-UV (panel B) wavelength ranges, and calculated the difference spectra between SPCp41 and S19P20s. The far-UV CD spectrum of S19P20s is very similar to that of the wild-type α-spectrin SH3 domain [8], which accords with the similarity in their structures [21,30], whilst the spectrum of SPCp41 has a larger negative ellipticity. The far-UV CD spectrum of isolated p41 is quite similar to those reported elsewhere for other proline-rich peptides in solution [31], compatible with a partial propensity to adopt a PPII helical conformation. In contrast, the difference spectrum between SPCp41 and S19P20s, which mainly characterises the backbone conformation of the chain extension, shows both in shape and intensity the typical characteristics of the CD spectrum of a PPII helix, with a positive band at 228 nm and a negative band at 204 nm [32,33]. This is consistent with the conformation usually observed for proline-rich peptides bound to SH3 domains and also found in the conformation of p41 in complex with Abl-SH3 [29].

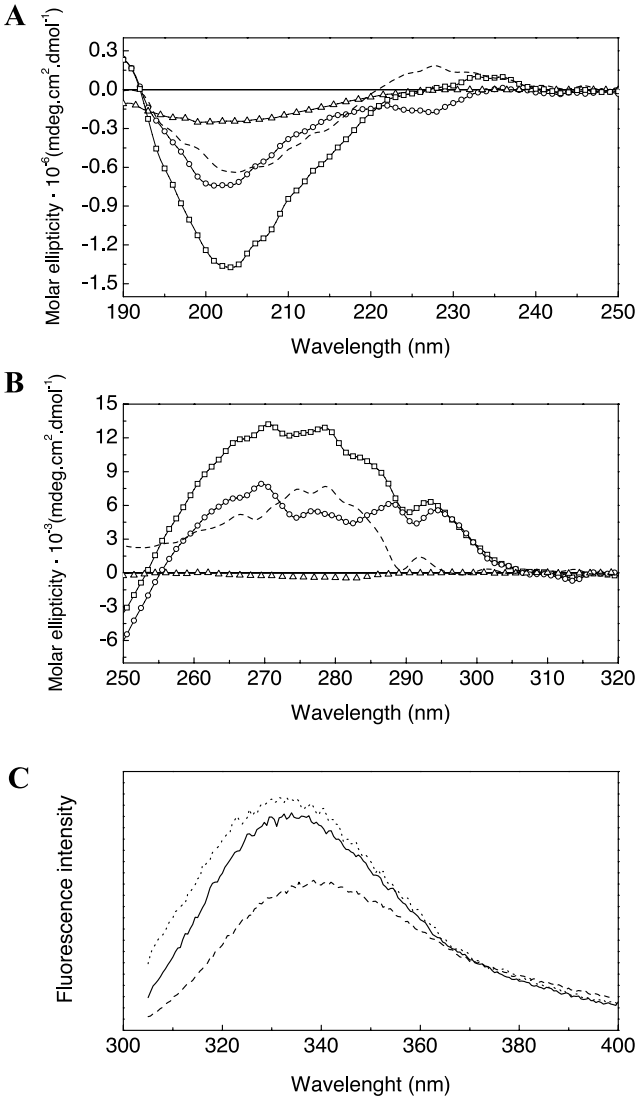

Fig. 2. A: Far-UV CD spectra of SPCp41 (squares), S19P20s (circles) and the isolated p41 decapeptide (triangles) in 20 mM glycine buffer, pH 3.0, 25°C. The dashed line represents the difference spectra between SPCp41 and S19P20s. B: Near-UV CD spectra for the same protein systems and conditions as those in panel A. Symbols and lines are also the same. C: Fluorescence spectra of SPCp41 (solid line), S19P20s (dashed line) and S19P20s in the presence of 1.5 mM of p41 (dotted line) under the same conditions as those of panels A and B. Excitation wavelength = 298 nm.

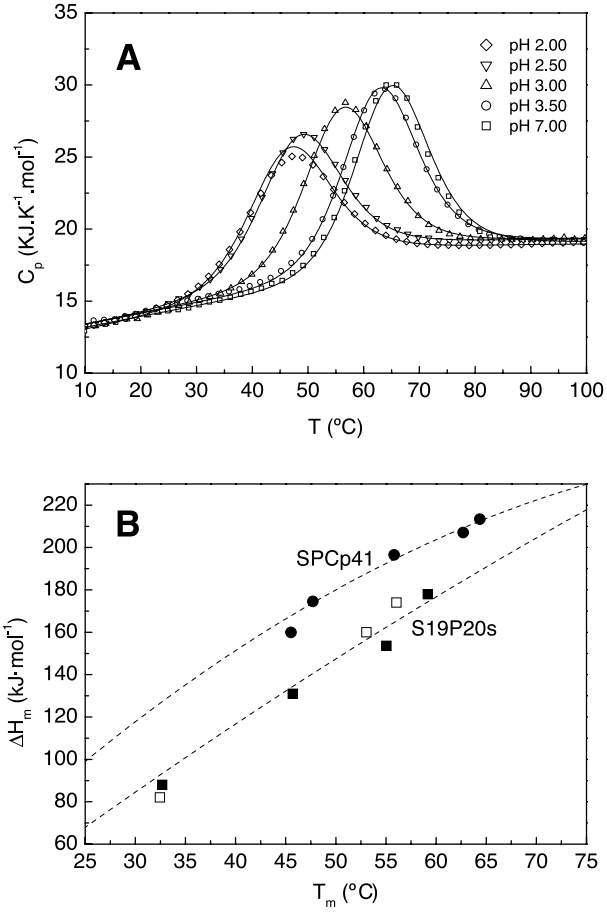

Fig. 3. A: Temperature dependence of the partial molar heat capacity, C_p, of SPCp41 at several pH values, as indicated in the plot. The experimental data are represented by open symbols. The solid lines represent the non-linear least-squares fitting to the whole set of C_p curves using the two-state unfolding model, in which the heat capacity functions for the native and the unfolded states (dashed lines) and the enthalpy change upon unfolding are considered to be independent of pH. B: Plot of the increase in enthalpy upon unfolding, ΔH_m, versus the unfolding temperature, T_m, for SPCp41 (circles) and S19P20s (squares). Open squares correspond to the data reported elsewhere for S19P20s [19]. The dashed lines represent the temperature dependence of the unfolding enthalpy obtained directly from the overall fittings using the two-state model.

The near-UV CD spectrum of SPCp41 has a clearly greater positive ellipticity than that of S19P20s. This difference is most pronounced at around 278 nm, which indicates the immobilisation of the tyrosine side chains in SPCp41 within the binding pocket of the SH3 motif due to contacts with the 13-residue extension, which accords well with the interactions observed between p41 and several aromatic residues of Abl-

SH3 in the crystal structure of the complex [29]. An additional, though smaller, difference in CD occurs at around 294 nm, indicating changes in the environment of a tryptophan side chain, most probably Trp24.

Titration of S19P20s with p41 monitored by tryptophan fluorescence produced a clear increase in intensity and a blue shift at the fluorescence spectrum's maximum, which was undoubtedly caused by the binding of p41 to the SH3 binding site (data not shown), as observed elsewhere for the Abl-SH3 domain [22]. This indicates that S19P20s is capable of binding the decapeptide p41, although with quite low affinity ($K_D = 160 \pm 34$ μM). The fluorescence spectrum of SPCp41, on the other hand, was completely unaffected by the addition of increasing amounts of p41, suggesting that the binding site was occupied by the extended sequence in the chimera. The fluorescence spectrum of SPCp41 was very similar to that of S19P20s saturated with p41 (Fig. 2C), indicating that the environments of Trp24 in the chimera SPCp41 and in the S19P20s–p41 complex are very similar.

We made a more detailed characterisation of the thermal unfolding of SPCp41 by DSC. Fig. 3A shows the heat-capacity profiles, C_p, obtained at different pH values between 2.0 and 7.0. The curves were fitted using the two-state unfolding model with the same method employed previously for the analysis of the DSC curves of the circular permutant S19P20s [19]. The quality of the fitting indicates that SPCp41 unfolds in a two-state process under all the conditions investigated. This result also reveals that the interactions between the SH3 motif and the p41 sequence are highly cooperative with the rest of the domain's structure.

For comparison, we made additional DSC experiments with S19P20s under the same conditions used for SPCp41. Table 1 shows the thermodynamic parameters of the unfolding of these two proteins at different pH values. The unfolding parameters for S19P20s are similar to those found in a previous work [19]. Fig. 3B shows the correlation between the unfolding enthalpy, ΔH_m, and the transition temperature, T_m, for both proteins. It is clear from the plot that the unfolding processes of the two proteins have quite different enthalpy functions, the unfolding enthalpy of the chimeric protein being significantly higher than that of S19P20s. The difference in enthalpy between the two correlations was about 32 kJ mol^{-1} at 50°C and hardly changed with temperature (Fig. 3B). This difference with opposite sign would account for the net enthalpy balance of the interactions between the p41 sequence and the SH3 binding site. This enthalpy is of similar magnitude and sign to the enthalpy of binding of the isolated p41 decapeptide to the wild-type α-spectrin SH3 domain measured directly by ITC (results not shown) and is also similar to the enthalpies found for the binding of other proline-rich peptides to different SH3 domains [6,7], which implies that the contribution of new interactions involving the cross-link sequence to the enthalpy of unfolding of SPCp41 is negligible.

Table 1
Thermodynamic parameters for the unfolding of SPCp41 and S19P20s deriving from an analysis of the DSC curves according to the two-state unfolding model

pH	Protein	T_m (°C)	ΔH_m (kJ mol^{-1})	ΔG_U (25°C) (kJ mol^{-1})
2.0	S19P20s	–	–	–
	SPCp41	45.5 ± 0.1	160 ± 1	8.5 ± 0.6
2.5	S19P20s	32.7 ± 0.6	88 ± 3	1.9 ± 0.3
	SPCp41	47.7 ± 0.1	175 ± 1	10.2 ± 0.7
3.0	S19P20s	45.7 ± 0.3	131 ± 2	6.3 ± 0.7
	SPCp41	55.8 ± 0.1	197 ± 1	14.6 ± 1.2
3.5	S19P20s	55.1 ± 0.3	154 ± 2	9.6 ± 1.2
	SPCp41	62.7 ± 0.1	207 ± 1	17.5 ± 1.7
7.0	S19P20s	59.2 ± 0.2	178 ± 2	12.5 ± 1.4
	SPCp41	64.4 ± 0.1	213 ± 1	18.6 ± 1.8

The thermal unfolding of SPCp41 and S19P20s was also followed by CD both in the far-UV and near-UV wavelength ranges at pH 3.0 (results not shown). All the unfolding profiles are very well described by the two-state model with equal enthalpy and T_m values in the two wavelength ranges and also very similar to those found by DSC, which confirms the two-state character of the unfolding of both proteins.

Table 1 includes the calculated Gibbs energy of unfolding for SPCp41 and S19P20s at 25°C. The difference in stability at 25°C between both species varies between 6.1 and 8.3 kJ mol^{-1}, depending upon the pH. This would in principle be related to the Gibbs energy balance upon the severing of the interactions between the extended sequence and the binding motif in SPCp41.

From the Gibbs energy of folding of S19P20s ($\Delta G^0_{fold,SH3} = -6.4 \pm 0.7$ kJ mol^{-1}) and the standard Gibbs energy of binding of p41 to S19P20s ($\Delta G^0_{bind} = -21.7 \pm 0.5$ kJ mol^{-1}), both at pH 3.0 and 25°C, the Gibbs energy of folding and docking of the S19P20s-p41 complex at 1 M standard state can be estimated as: $\Delta G^0_{chimera} = \Delta G^0_{fold,SH3} + \Delta G^0_{bind}$, which is equal to -28.1 ± 1.2 kJ mol^{-1}. Compared to this, and assuming the absence of enthalpy effects produced by cross-linking, as referred to above, the Gibbs energy of folding of SPCp41 (-14.6 ± 1.2 kJ mol^{-1}) can be expressed as: $\Delta G^0_{chimera} = \Delta G^0_{fold,SH3} + \Delta G^0_{bind} - T\Delta S^0_{link}$, where the last quantity is the contribution to the stability of the system arising from the change in configurational entropy upon the insertion of the three-residue link between the two polypeptide chains. The subtraction of these two Gibbs energy values allows us to estimate $-T\Delta S^0_{link}$, which is equal to 13.5 ± 2.4 kJ mol^{-1}. According to this calculation, the introduction of the cross-link would add a large unfavourable entropic term to the stability of the chimera SPCp41 compared to that of the complex between S19P20s and p41. The entropic contribution of introducing a six-residue cross-link in a dimeric system of two associating helices has recently been calculated theoretically [34]. The authors also report a similar entropic destabilisation (13.4 kJ mol^{-1}) upon cross-linking the helices at 1 M standard state and 300 K. This paradoxical result appears to arise from the fact that these magnitudes correspond to the 1 M standard state concentration, which is unrealistically high for macromolecules. For a more realistic reference state (1 μM concentration of reagents) the entropic contribution deriving from cross-linking the helices becomes strongly stabilising (-21 kJ mol^{-1}), as might be expected.

In our system, using as reference state a concentration of reactants of 50 μM, similar to that of the titration experiments, the Gibbs energy of binding between p41 and S19P20s, ΔG_{bind}, is 2.8 ± 1.2 kJ mol^{-1}, indicating that at this reference concentration the complex is intrinsically unstable. Under these conditions, $-T\Delta S_{link}$ is calculated as -11.0 ± 2.4 kJ mol^{-1}, which is comparable to the values reported theoretically and experimentally for other systems [34]. Therefore, the cross-link adds extra stability to the interactions at the

binding interface within the chimera SPCp41, which in turn behaves as a two-state unfolding protein.

In spite of this two-state behaviour, the thermodynamic magnitudes of unfolding of SPCp41 are strongly biased by the thermodynamics of the interactions between the SH3 motif and the p41 sequence, as can be seen in Table 1. Therefore, with all other factors constant, changes in these interactions will be reflected in changes in the thermodynamic parameters of unfolding of the chimera, quantifiable by DSC.

We conclude that the chimeric protein described in this work mimics the structural and energetic features of the binding process between the SH3 domain and the ligand p41, with a PPII helix conformation for the p41 sequence, a similar immobilisation of aromatic residues at the binding interface and an interaction enthalpy at the interface analogous to that reported for the binding of proline-rich peptides to other SH3 domains.

There are two comparable examples in the literature of the intra-molecular binding of a proline-rich sequence to an adjacent SH3 domain, one being part of the natural regulatory mechanism of the T-cell-specific kinase ITK [35] and the other an artificial fusion between the Hck-SH3 domain and a proline-rich sequence of human GAP [36]. In these proteins, however, the proline-rich sequences were connected by a long polypeptide segment to the N- and C-terminus of the SH3 motif, respectively. The SPCp41 chimera, on the other hand, has a novel topology and a very short link of three residues, as a result of using a circular permutant of the SH3 domain, thus bringing its C-terminus very close to the binding site. In all cases the ligand sequence occupies intra-molecularly the binding site favoured by the removal of configurational entropy for the bi-molecular binding reaction. One of the reasons for the high unfolding cooperativity of SPCp41 may be the shortness of the link, which would result in a relatively small conformational entropy loss upon the immobilisation of the extended sequence at the binding site. Consequently, the thermal unfolding of this chimera agrees with a simple two-state process, which is easy to characterise energetically by typical unfolding experiments such as DSC.

In addition to a general interest in the design of these chimeric constructions in protein folding, the possibility also exists of their being used as tools to optimise interactions at the binding site of SH3 by site-directed mutagenesis and simple stability measurements. This may short-cut the traditionally inefficient and expensive procedures used until now to design peptides with improved affinity and specificity for SH3 domains.

Acknowledgements: This work has been financed by Grants HPRN-CT-2002-00241 from the European Union and BIO2000-1459 from the Spanish Ministry of Science and Technology. We also thank Dr. J. Trout for revising the English text.

References

[1] Mayer, B.J. (2001) J. Cell Sci. 114, 1253–1263.
[2] Kay, B.K., Williamson, M.P. and Sudol, M. (2000) FASEB J. 14, 231–241.
[3] Leavitt, S. and Freire, E. (2001) Curr. Opin. Struct. Biol. 11, 560–566.
[4] Arold, S.T., Ulmer, T.S., Mulhern, T.D., Werner, J.M., Ladbury, J.E., Campbell, I.D. and Noble, M.E. (2001) J. Biol. Chem. 276, 17199–17205.
[5] Ferreon, J.C. and Hilser, V.J. (2003) Protein Sci. 12, 447–457.
[6] Lemmon, M.A., Ladbury, J.E., Mandiyan, V., Zhou, M. and Schlessinger, J. (1994) J. Biol. Chem. 269, 31653–31658.
[7] Wang, C., Pawley, N.H. and Nicholson, L.K. (2001) J. Mol. Biol. 313, 873–887.
[8] Viguera, A.R., Martinez, J.C., Filimonov, V.V., Mateo, P.L. and Serrano, L. (1994) Biochemistry 33, 2142–2150.
[9] Grantcharova, V.P. and Baker, D. (1997) Biochemistry 36, 15685–15692.
[10] Grantcharova, V.P., Riddle, D.S., Santiago, J.V. and Baker, D. (1998) Nat. Struct. Biol. 5, 714–720.
[11] Martinez, J.C., Pisabarro, M.T. and Serrano, L. (1998) Nat. Struct. Biol. 5, 721–729.
[12] Plaxco, K.W., Guijarro, J.I., Morton, C.J., Pitkeathly, M., Campbell, I.D. and Dobson, C.M. (1998) Biochemistry 37, 2529–2537.
[13] Guijarro, J.I., Morton, C.J., Plaxco, K.W., Campbell, I.D. and Dobson, C.M. (1998) J. Mol. Biol. 276, 657–667.
[14] Martinez, J.C. and Serrano, L. (1999) Nat. Struct. Biol. 6, 1010–1016.
[15] Riddle, D.S., Grantcharova, V.P., Santiago, J.V., Alm, E., Ruczinski, I. and Baker, D. (1999) Nat. Struct. Biol. 6, 1016–1024.
[16] Ding, F., Dokholyan, N.V., Buldyrev, S.V., Stanley, H.E. and Shakhnovich, E.I. (2002) Biophys. J. 83, 3525–3532.
[17] Shea, J.E., Onuchic, J.N. and Brooks, C.L. (2002) Proc. Natl. Acad. Sci. USA 99, 16064–16068.
[18] Borreguero, J.M., Dokholyan, N.V., Buldyrev, S.V., Shakhnovich, E.I. and Stanley, H.E. (2002) J. Mol. Biol. 318, 863–876.
[19] Martinez, J.C., Viguera, A.R., Berisio, R., Wilmanns, M., Mateo, P.L., Filimonov, V.V. and Serrano, L. (1999) Biochemistry 38, 549–559.
[20] Gsponer, J. and Caflisch, A. (2001) J. Mol. Biol. 309, 285–298.
[21] Viguera, A.R., Serrano, L. and Wilmanns, M. (1996) Nat. Struct. Biol. 3, 874–880.
[22] Pisabarro, M.T. and Serrano, L. (1996) Biochemistry 35, 10634–10640.
[23] Kunkel, T.A. (1985) Proc. Natl. Acad. Sci. USA 82, 488–492.
[24] Peranen, J., Rikkonen, M., Hyvonen, M. and Kaariainen, L. (1996) Anal. Biochem. 236, 371–373.
[25] Sadqi, M., Casares, S., Abril, M.A., Lopez-Mayorga, O., Conejero-Lara, F. and Freire, E. (1999) Biochemistry 38, 8899–8906.
[26] Gill, S.C. and Vonhippel, P.H. (1989) Anal. Biochem. 182, 319–326.
[27] Cobos, E.S., Filimonov, V.V., Galvez, A., Valdivia, E., Maqueda, M., Martinez, J.C. and Mateo, P.L. (2002) Biochim. Biophys. Acta 1598, 98–107.
[28] Guex, N. and Peitsch, M.C. (1997) Electrophoresis 18, 2714–2723.
[29] Pisabarro, M.T., Serrano, L. and Wilmanns, M. (1998) J. Mol. Biol. 281, 513–521.
[30] Musacchio, A., Noble, M., Pauptit, R., Wierenga, R. and Saraste, M. (1992) Nature 359, 851–855.
[31] Viguera, A.R., Arrondo, J.L., Musacchio, A., Saraste, M. and Serrano, L. (1994) Biochemistry 33, 10925–10933.
[32] Manning, M.C. and Woody, R.W. (1991) Biopolymers 31, 569–586.
[33] Rabanal, F., Ludevid, M.D., Pons, M. and Giralt, E. (1993) Biopolymers 33, 1019–1028.
[34] Zaman, M.H., Berry, R.S. and Sosnick, T.R. (2002) Proteins 48, 341–351.
[35] Andreotti, A.H., Bunnell, S.C., Feng, S., Berg, L.J. and Schreiber, S.L. (1997) Nature 385, 93–97.
[36] Gmeiner, W.H., Xu, J.Z., Horita, D.A., Smithgall, T.E., Engen, J.R., Smith, D.L. and Byrd, R.A. (2001) Cell. Biochem. Biophys. 35, 115–126.